Molecular Vision 2016; 22:116-128 <http://www.molvis.org/molvis/v22/116>
Received 6 November 2015 | Accepted 1 February 2016 | Published 3 February 2016

TNF-α mediates choroidal neovascularization by upregulating VEGF expression in RPE through ROS-dependent β-catenin activation

Haibo Wang,[1] Xiaokun Han,[1,3] Erika S. Wittchen,[2] M. Elizabeth Hartnett[1]

[1]The John Moran Eye Center, University of Utah, Salt Lake City, UT; [2]Cell Biology and Physiology, University of North Carolina at Chapel Hill, Chapel Hill, NC; [3]Department of Ophthalmology, The Fourth Affiliated Hospital of China Medical University, Shenyang, China

Purpose: Inflammation, oxidative stress, and angiogenesis have been proposed to interact in age-related macular degeneration. It has been postulated that external stimuli that cause oxidative stress can increase production of vascular endothelial growth factor (VEGF) in retinal pigment epithelial (RPE) cells. In this study, we tested the hypothesis that the inflammatory cytokine, tumor necrosis factor alpha (TNF-α), contributed to choroidal neovascularization (CNV) by upregulating VEGF in RPE through intracellular reactive oxygen species (ROS)-dependent signaling and sought to understand the mechanisms involved.

Methods: In a murine laser-induced CNV model, 7 days after laser treatment and intravitreal neutralizing mouse TNF-α antibody or isotype immunoglobulin G (IgG) control, the following measurements were made: 1) TNF-α protein and VEGF protein in RPE/choroids with western blot, 2) CNV volume in RPE/choroidal flatmounts, and 3) semiquantification of oxidized phospholipids stained with E06 antibody within CNV with immunohistochemistry (IHC). In cultured human RPE cells treated with TNF-α or PBS control, 1) ROS generation was measured using the 2',7'-dichlorodihydrofluorescein diacetate (DCFDA) fluorescence assay, and 2) NOX4 protein and VEGF protein or mRNA were measured with western blot or quantitative real-time PCR in cells pretreated with apocynin or nicotinamide adenine dinucleotide phosphate-oxidase (NADPH) inhibitor, VAS 2870, or transfected with p22phox siRNA, and each was compared to its appropriate control. Western blots of phosphorylated p65 (p-p65), total p65 and β-actin, and quantitative real-time PCR of VEGF mRNA were measured in human RPE cells treated with TNF-α and pretreatment with the nuclear factor kappa B inhibitor, Bay 11–7082 or control. Western blots of β-catenin, VEGF, and p22phox and coimmunoprecipitation of β-catenin and T-cell transcriptional factor were performed in human RPE cells treated with TNF-α following pretreatment with β-catenin transcriptional inhibitors, XAV939 or JW67, or transfection with p22phox siRNA and compared to appropriate controls.

Results: Compared to the non-lasered control, TNF-α and VEGF protein were increased in the RPE/choroids in a murine laser-induced CNV model ($p<0.05$). An intravitreal neutralizing antibody to mouse TNF-α reduced CNV volume, and VEGF protein in the RPE/choroids ($p<0.01$) and oxidized phospholipids within CNV compared to IgG control ($p<0.05$). In cultured RPE cells and compared to controls, TNF-α induced ROS generation and increased activation of NOX4, an isoform of NADPH oxidase; both were prevented by pretreatment with the apocynin or VAS2870 or knockdown of p22phox, a subunit of NADPH oxidase. TNF-α treatment increased VEGF expression ($p<0.001$) and the formation of a transcriptional complex of β-catenin and T-cell transcriptional factor; both were prevented by pretreatment with apocynin or knockdown of p22phox. Inhibition of β-catenin by XAV939, but not the nuclear factor kappa B inhibitor, Bay 11–7082, prevented TNF-α-induced VEGF upregulation.

Conclusions: Our results support the thinking that TNF-α contributes to CNV by upregulating VEGF production in RPE cells through ROS-dependent activation of β-catenin signaling. These results provide mechanisms of crosstalk between inflammatory mediator, TNF-α, and ROS in RPE cells.

Neovascular age-related macular degeneration (AMD) is a leading cause of central vision loss in the elderly [1,2], AMD is a complex disease in that it involves multiple different cell types and many signaling pathways, including those involving oxidation, inflammation, and angiogenesis [3-6]. Currently, antiangiogenic agents that interfere with the bioactivity of vascular endothelial growth factor (VEGF) are the standard of care for neovascular AMD based on evidence from human clinical trials [7,8], but these agents are effective in about 40% of eyes. There are several potential reasons for this, and one is that other factors, such as those involved in oxidative or inflammatory signaling mechanisms, are also important and may be playing a role in the pathophysiology. Experimental animal models of neovascular AMD induced

Correspondence to: M. Elizabeth Hartnett, 65 N. Mario Capecchi Drive, Salt Lake City, UT 84132; Phone: (801) 213-4044; FAX: (801) 581-3357; email: ME.Hartnett@hsc.utah.edu

by laser show reduced, but not abolished, choroidal neovascularization (CNV) from antioxidants or through silencing or knockout of genes involved in oxidative signaling [9,10]. Antioxidants also slow the progression of AMD in human clinical trials [11].

In animal models of laser-induced CNV, macrophages recruited to the outer retina release inflammatory cytokines to contribute to CNV volume [12]. Macrophages release inflammatory cytokines that have been found in human specimens of advanced AMD [13,14]. However, the evidence for inhibiting inflammation broadly through steroids or inhibitors of cytokines, is less clear [15-17].

The cytokine, tumor necrosis factor alpha (TNF-α), has been associated with advanced forms of AMD [14]. Elevated systemic TNF-α was found in patients with AMD and a variant of the complement factor (CFH) Y402H polymorphism, which is highly correlated with AMD [13]. In neovascular AMD, TNF-α was found in macrophages within surgically removed CNV from patients with neovascular AMD [14]. TNF-α and reactive oxygen species (ROS) have been associated with CNV in laser-induced models [3]. However, in vitro, TNF-α decreased VEGF secretion in a highly polarized layer of RPE cells with intact barriers, and only increased VEGF expression in non-polarized RPE cells, which had reduced barrier integrity [18]. To gain insight into the interactions between oxidative and inflammatory signaling on RPE cell-induced VEGF expression and the development of CNV, we tested the hypothesis that TNF-α upregulates VEGF expression in RPE cells via ROS-dependent signaling. We found that TNF-α activated NADPH oxidase to generate ROS that then triggered β-catenin transcriptional activation to increase VEGF expression in RPE cells and in a laser-induced CNV model.

METHODS

Animals: Five- to eight-week-old C57Bl/6 wild-type mice were used in these studies. All animal procedures were conducted in accordance with the University of Utah Guide for the Care and Use of Laboratory Animals and the Association for Research in Vision and Ophthalmology Statement for the Use of Animals in Ophthalmic and Vision Research.

Laser-induced CNV model and injections: The laser-induced CNV model was performed as previously described [10]. Intraperitoneal injections of 100 mg/kg ketamine (Hospira, Inc., Lake Forest, IL) and 20 mg/kg xylazine (AnaSed Lloyd Laboratories, Shenandoah, IA) were used for anesthesia. Following mydriasis with 1% tropicamide ophthalmic solution (Bausch & Lomb, Tampa, FL), the mouse was secured on a stage, and a coupling agent, GenTeal (Alcon, Fort Worth, TX), was applied to the cornea. Laser photocoagulation was performed with a 532 nm Phoenix Image-Guided Laser System (Phoenix Micron IV, Pleasanton, CA) using the settings of 400 mW intensity and 100 ms duration. Four to five laser spots per eye were applied approximately 2 disc diameters from the optic nerve, avoiding major vessels. Disruption of Bruch's membrane was confirmed by the appearance of a cavitation bubble. Right after laser injury, using a MICROLITER syringe (Hamilton Company, Reno, NV), an intravitreal injection of total volume of 1 µl of neutralizing anti-mouse TNF-α antibody (TNF-α Ab, 50 ng/ml, R&D Systems, Minneapolis, MN) or control, isotype immunoglobulin G (IgG, 50 ng/ml, R & D Systems). Both eyes of each mouse were lasered and injected with the same type of injection. Seven days after the laser treatment, the mice were euthanized by CO_2 exposure, and one eye from each mouse was collected for RPE/choroidal flatmount analysis and the fellow eye for protein by immunostaining of the retinal cryosections or western blot analysis. Each group included both eyes of at least eight mice.

Analysis of CNV volume in RPE/choroidal flatmounts: Eyes were first fixed in 4% paraformaldehyde (Electron Microscopy Sciences [EMS], Hatfield, PA) for 1 h. After the cornea was removed, the lens, retina and vitreous, and posterior eyecups of the RPE/choroid/sclera were dissected. The eyecups were stained with Alexa Fluor 568-conjugated isolectin B4 (Invitrogen, Carlsbad, CA, Cat # I21412) overnight at 4 °C to label invading choroidal vessels. The eyecups were then flattened by cutting radial incisions and flatmounted on a microscope slide with Fluoromount G (Southern Biotech, Birmingham, AL) for confocal imaging. The flatmounts were imaged by taking optical Z-sections at3 µm increments with a confocal microscope (FV1000, Olympus, Melville, NY). The volume ($µm^3$) of each lesion of CNV was measured by computerized image analysis using software provided with the microscope. Lesions with obvious hemorrhage or bridging CNV were excluded. Each CNV spot was considered an independent data point. For each condition, at least 30 spots were analyzed from eight mice.

Retinal and RPE/choroidal section preparation and immunostaining of OxPLs: Eyes were first fixed in 4% paraformaldehyde for 1 h, and then the corneas and lenses were removed. Eyecups were incubated in 30% sucrose overnight and frozen at −80 °C after immersion in optimal cutting temperature compound (OCT: Tissue Tek; EMS). The eyecups were cut into 12 µm cryosections. Sections were incubated with E06 monoclonal antibody (1:100, Avanti POLAR LIPIDS, Inc., Alabaster, Alabama, Cat # 330001) overnight at 4 °C. After rinsing, the sections were incubated for 1 h with fluorescein

isothiocyanate (FITC)-conjugated goat anti-mouse IgM (1:100, Sigma-Aldrich, St. Louis, MO, Cat # F9259), Alexa Fluor 568-conjugated antibody for isolectin B4 (lectin, 1:200, Invitrogen) to stain the vessels, and Topro 3 (1:1,000, Life Technologies, Grand Island, NY) to stain the nuclei. The sections stained with no primary antibody were used as controls. Labeling for all sections was performed during the same experimental session. Images were captured using confocal microscopy (Olympus IX81) at 20X magnification. Within the sections of lectin-stained CNV, E06 labeling to measure oxidized phospholipids (OxPLs) was determined with fluorescent density using Image J. At least ten CNV lesions per condition were analyzed (n=6 per condition).

Cell culture: Human primary RPE cells (hRPE; Lonza, Walkersville, MD) were grown in retinal pigment epithelial cell basal media (RtEBM, Lonza) and used from passages 3–5. In some experiments, the cells were pretreated with the nuclear factor kappa B (NF-κB) inhibitor, Bay 11–7082 (5 μM), or Wnt/beta catenin inhibitors, JW 67 (20 μM) or XAV939 (1 μM; Tocris Bioscience, Bristol, UK), and then incubated with human recombinant TNF-α (20 ng/ml, R&D Systems) or PBS (1X, 137.93 mM NaCl, 8.06 mM $NaPO_4$, 2.67 mM KCl, 1.47 mM KH_2PO_4, pH 7.4) for further analyses.

siRNA transfection in human RPE cells: To knock down p22phox, RPE cells were transfected using Lipofectamine 2000 according to the commercial protocol (Life Technologies) with siRNA targeting the human *CYBA* gene (Gene ID: 1535 and OMIM 608508; p22phox) or silencer selective negative control siRNA (both from Life Technologies). Forty-eight hours after transfection, the cells were incubated with human recombinant TNF-α (20 ng/ml, R&D Systems) or PBS for further analysis. All experimental conditions were plated in triplicate.

ROS generation assay in human RPE cells: RPE cells were seeded into 96-well plates and infected with adenoviral constructs. Forty-eight hours post infection, the cells were loaded with 5 μM 2',7'-dichlorofluorescein diacetate (DCFDA, Invitrogen) in serum-free medium for 30 min at 37 °C. After two washes with PBS, the cells were pretreated with apocynin (100 μM), or NADPH oxidase inhibitor, VAS 2870 (20 μM, EMD Millipore), or control PBS or dimethyl sulfoxide (DMSO) for 30 min and then incubated with TNF-α or control PBS for another 30 min. ROS generation was measured in a fluorescent plate reader (excitation at 488 nm and emission at 520 nm). Cells incubated with 10 μM H_2O_2 were used as a positive control (n=9 per condition).

Immunoprecipitation and immunoblots: RPE cells were lysed in radioimmunoprecipitation assay buffer (RIPA) with protease inhibitor cocktail (Roche Diagnostics, Indianapolis, IN) and orthovanadate (Sigma-Aldrich). Lysates were clarified with centrifugation at $1.61x10^4$ ×g for 5 min at 4 °C. The protein concentration in the supernatant was quantified with bicinchoninic acid assay (BCA; Pierce, Rockford, IL). The total protein (500 μg in 500 μl) for each sample was incubated with antibody to T cell factor 1 (TCF1, 1:200, Cell Signaling Technology Inc., Danvers, MA) by gently rocking at 4 °C overnight. Ten microliters of Dynabeads protein G (Invitrogen) were added and incubated for an additional 1 h at 4 °C. The antibody/protein/agarose complex was washed three times with RIPA buffer and resuspended in 2X sample buffer. The protein complex bound to TCF1 or pan-cadherin was separated with NuPAGE 4% to 12% Bis-Tris Gels (Invitrogen) and transferred to a polyvinylidene fluoride (PVDF) membrane, and then incubated with antibody to β-catenin (1:1,000, Cell Signaling Technology Inc.) overnight at 4 °C. All membranes were reprobed with TCF1 or pan-cadherin to ensure equal protein loading.

For TNF-α, VEGF and β-catenin in the RPE/choroids or in the RPE cells, 20 μg of protein from each treatment was loaded into NuPAGE 4% to 12% Bis-Tris Gels (Invitrogen), transferred to a PVDF membrane, and incubated with antibodies to TNF-α (1:1,000, Cell Signaling Technology Inc.), VEGF (1:500, Santa Cruz Biotechnology, Santa Cruz, CA), or β-catenin at 4 °C overnight. Densitometry analysis was performed on exposed films with the use of the software UN-SCAN-IT version 6.1 (Silk Scientific, Orem, UT). All experimental conditions were plated in triplicate (n=6).

RNA Isolation and qPCR analysis: Total RNA of the RPE/choroidal tissues was extracted with TRI Reagent (Sigma-Aldrich). RNA was quantified using a NanoDrop spectrophotometer (Thermo Fisher Scientific, Waltham, MA). cDNA was generated with the use of a high-capacity cDNA archive kit (Life Technologies). Quantitative PCR (qPCR) was performed on a Mastercycler ep realplex system (Eppendorf, Hauppauge, NY) with the use of SYBR Green Master Mix (Roche Diagnostics) and primers synthesized by the core research facility of the University of Utah. Expression levels for VEGF were normalized to the mean value of the internal control, GAPDH. The primers (forward and reverse, respectively) were mouse VEGF 5′-TGG TTC TTC ACT CCC TCA AAT C-3′ and 5′- GGT CTC TCT CTC TCT TCC TTG A-3′, and mouse GAPDH 5′-GGA GAA ACC TGC CAA GTA TGA-3′ and 5′-TCC TCA GTG TAG CCC AAG A-3′.

Statistical analysis: Significant differences between groups were determined with ANOVA with post hoc protection using the Bonferroni multiple comparison test. Results were the mean ± standard error of the mean (SEM). A minimum p value of less than 0.05 was considered statistically significant.

For animal studies, at least 30 laser spots were analyzed for CNV, and ten retinal sections, $p<0.01$ for oxidized phospholipids (OxPLs) from different animals. Western blot or PCR analyses included six to eight retinas/condition. For analysis of densitometry of the immunolabeled retinas, at least three sections imaged at 60 µm intervals were examined/eye. For IHC and western blots, a total of at least three (IHC) or five (western blots) eyes were analyzed for each condition. For in vitro studies, each experimental condition included an n=6–9, and each experiment was performed three times.

RESULTS

TNF-α mediates CNV formation in association with increased VEGF expression in a murine l laser-induced CNV model: TNF-α ($p<0.05$) and VEGF ($p<0.01$) protein in RPE/choroid lysates were significantly increased 7 days after laser injury compared to the non-lasered controls (Figure 1A,B). Similar to previous studies [19], treatment with intravitreal neutralizing antibody to mouse TNF-α (TNF-α Ab) significantly reduced the volume of laser-induced CNV compared to the mice treated with the isotype IgG control (IgG; Figure 1C,D, $p<0.01$) To determine if reduced CNV volume was associated with reduced VEGF, we measured the VEGF protein in the RPE/choroids by western blot and found that in the mice treated with intravitreal TNF-α Ab, VEGF protein in the RPE/choroids was significantly decreased compared to that in the RPE/choroids from the mice treated with intravitreal IgG (Figure 1E,F, $p<0.01$). These results provide evidence that TNF-α induced CNV was associated with increased VEGF expression.

TNF-α induces NADPH oxidase-generated ROS at CNV lesions and in cultured RPE cells: We previously found that external sources of oxidative stress were implicated in laser-induced CNV [10,20]. Therefore, we determined the effect of TNF-α on ROS generation in laser-induced CNV. We measured OxPLs by immunostaining with the E06 antibody. As shown in Figure 2A, OxPL staining was located within CNV, and quantification of immunofluorescence confirmed that OxPL staining was significantly reduced in the TNF-α Ab-treated mice compared to the control IgG-treated mice (Figure 2B, $p<0.05$). Additionally, ROS generation was measured with 2',7'-dichlorofluorescein diacetate (DCFDA) fluorescence in cultured human RPE cells incubated with different doses of recombinant human TNF-α for 30 min. Compared to PBS, TNF-α significantly increased ROS generation in a dose-dependent pattern (Figure 3A). To determine whether TNF-α-mediated ROS generation involved activation of NADPH oxidase, ROS were measured in RPE cells pretreated with apocynin (Apo) or the NADPH oxidase inhibitor, VAS2870 (VAS), for 30 min before stimulation with TNF-α. As shown in Figure 3B, pretreatment with Apo or VAS prevented TNF-α-induced ROS generation ($p<0.001$). We previously reported that NOX2 was involved in CNV pathogenesis, as evidenced by reduced CNV in laser-treated p47phox knockout mice compared to the wild-type mice [10]. We also found that VEGF-activated NOX4, an isoform of NADPH oxidase, mediated retinal microvascular endothelial cell proliferation by interacting with VEGFR2 [21]. Therefore, we determined whether TNF-α activated NOX4 in RPE cells. The NOX4 protein level and activation determined by cobinding with p22phox were measured in RPE cells treated with TNF-α or PBS, and VEGF was used as a positive control. As shown in Figure 3, compared to PBS, overnight treatment with TNF-α increased the NOX4 protein level (Figure 3C) and activation (Figure 3D,E, $p<0.05$). NADPH oxidase-dependent ROS generation was further determined in the RPE cells transfected with siRNA targeting human p22phox, a subunit required for NADPH oxidase activation by NOX2 or NOX4. Compared to the control siRNA and PBS treatment, knockdown of p22phox prevented ROS generation in RPE cells treated with PBS $p<0.05$ or TNF-α ($p<0.001$; Figure 3F). These results provide evidence that activation of NADPH oxidase was likely a source of ROS generation in the RPE cells and that TNF-α-mediated ROS in the RPE cells was generated through activation of NADPH oxidase.

TNF-α upregulates VEGF expression in RPE cells via ROS-dependent activation of β-catenin: To determine whether TNF-α affects VEGF expression in RPE cells, VEGF was measured with western blot after treatment of the RPE cells with TNF-α for 0, 3, 6, or 12 h. As shown in Figure 4A, TNF-α increased VEGF protein level as early as 3 h after TNF-α treatment and remained upregulated at 12 h compared to control. To determine whether ROS signaling was involved in TNF-α-mediated VEGF upregulation, RPE cells were pretreated with apocynin for 30 min to quench ROS before incubation with TNF-α overnight and then analyzed for VEGF mRNA with quantitative PCR. TNF-α-induced VEGF mRNA was significantly inhibited by apocynin treatment (Figure 4B, $p<0.05$), suggesting that TNF-α upregulates VEGF expression in RPE cells via ROS-dependent signaling.

Activation of NF-κB is a classic inflammatory signaling pathway mediated by TNF-α. Therefore, we tested whether inhibition of NF-κB would inhibit TNF-α-mediated VEGF expression in RPE cells. In RPE cells, TNF-α activated NF-κB determined by increased p-p65, but inhibition of TNF-α-induced NF-κB activation by Bay 11–7082 (Figure 5A) did not affect TNF-α-induced VEGF upregulation

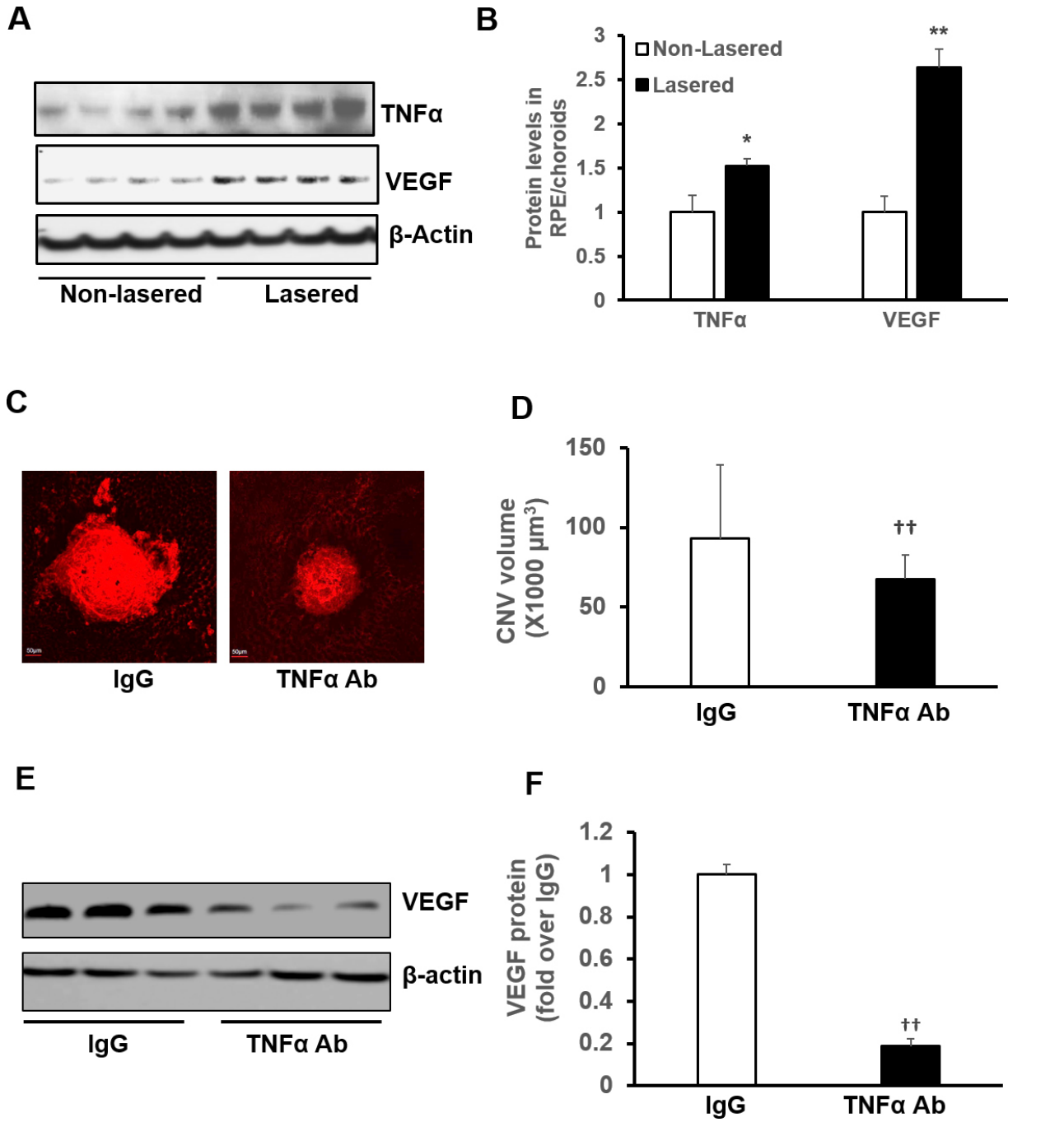

Figure 1. TNF-α mediates CNV formation in association with VEGF expression in a murine model of laser-induced CNV. **A**: Representative images of western blot of tumor necrosis factor alpha (TNF-α) and vascular endothelial growth factor (VEGF) protein in RPE/choroids of C57Bl/6 6-week-old mice without laser treatment (non-lasered) or 7 days after laser treatment. **B**: Quantification of densitometry (lasered; *p<0.05, **p<0.01 versus non-lasered). **C**: Representative images of choroidal neovascularization (CNV) volume. **D**: Quantification of CNV volume. **E**: Representative images of western blot of VEGF in RPE/choroids of mice injected with isotype immunoglobulin G (IgG, 50 ng) or neutralizing TNF-α antibody. **F**: Quantification of densitometry (TNF-α Ab, 50 ng; ††p<0.01 versus IgG).

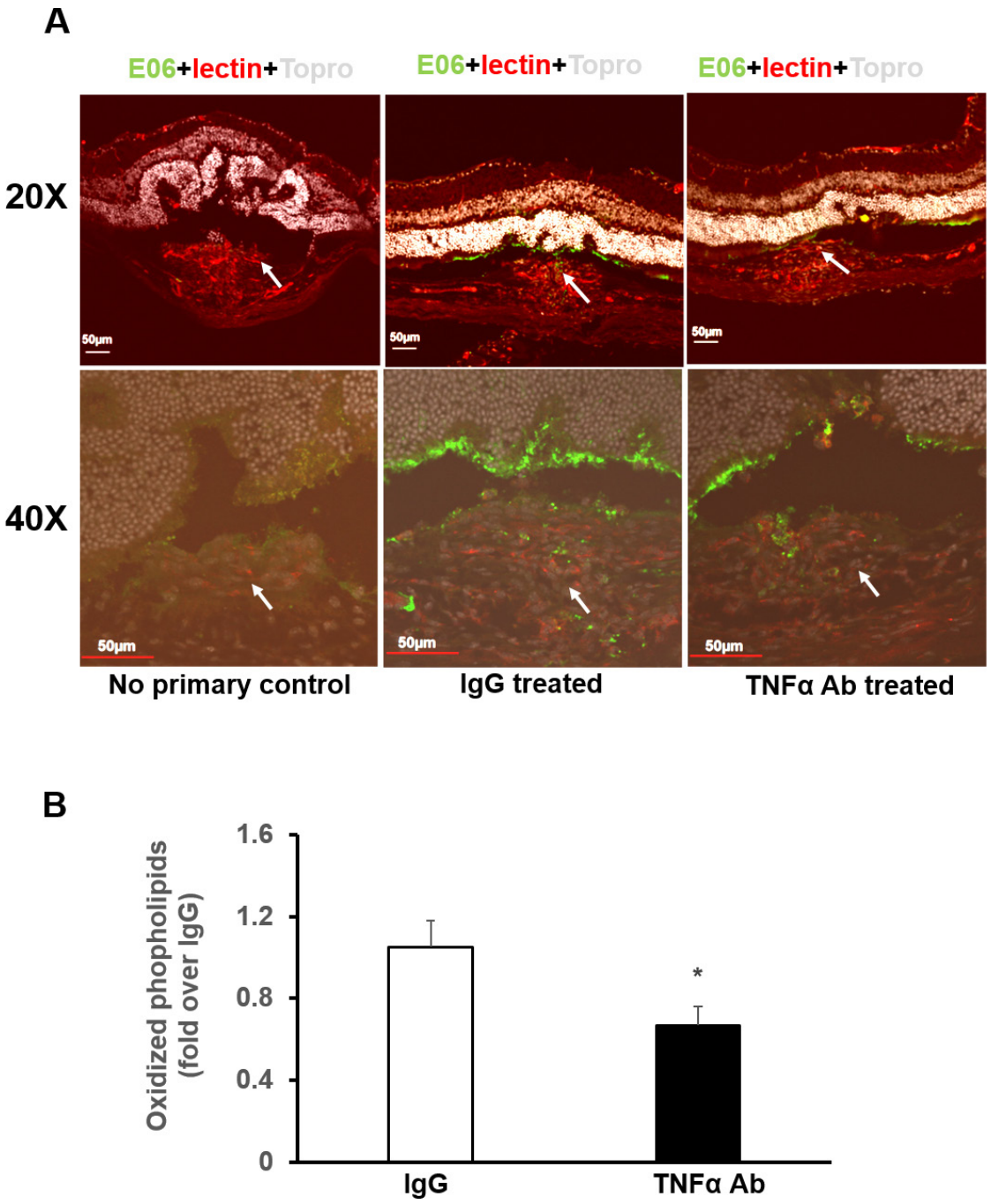

Figure 2. TNF-α induces ROS generation within multiple cell types within CNV lesions. **A**: Immunostaining for oxidized phospholipids (OxPLs) in retinal/choroidal cryosections. Images were taken in the regions with choroidal neovascularization (CNV) at 20X and 40X magnification. Top panel: 20X, bottom panel: 40X. Green, OxPL; Red, lectin; Gray, Topro 3. **B**: Quantification of densitometry of OxPL immunofluorescence at CNV lesions of mice injected with isotype immunoglobulin G (IgG, 50 ng) or neutralizing tumor necrosis factor alpha (TNF-α) antibody (TNF-α Ab, 50 ng; *p<0.05 versus IgG).

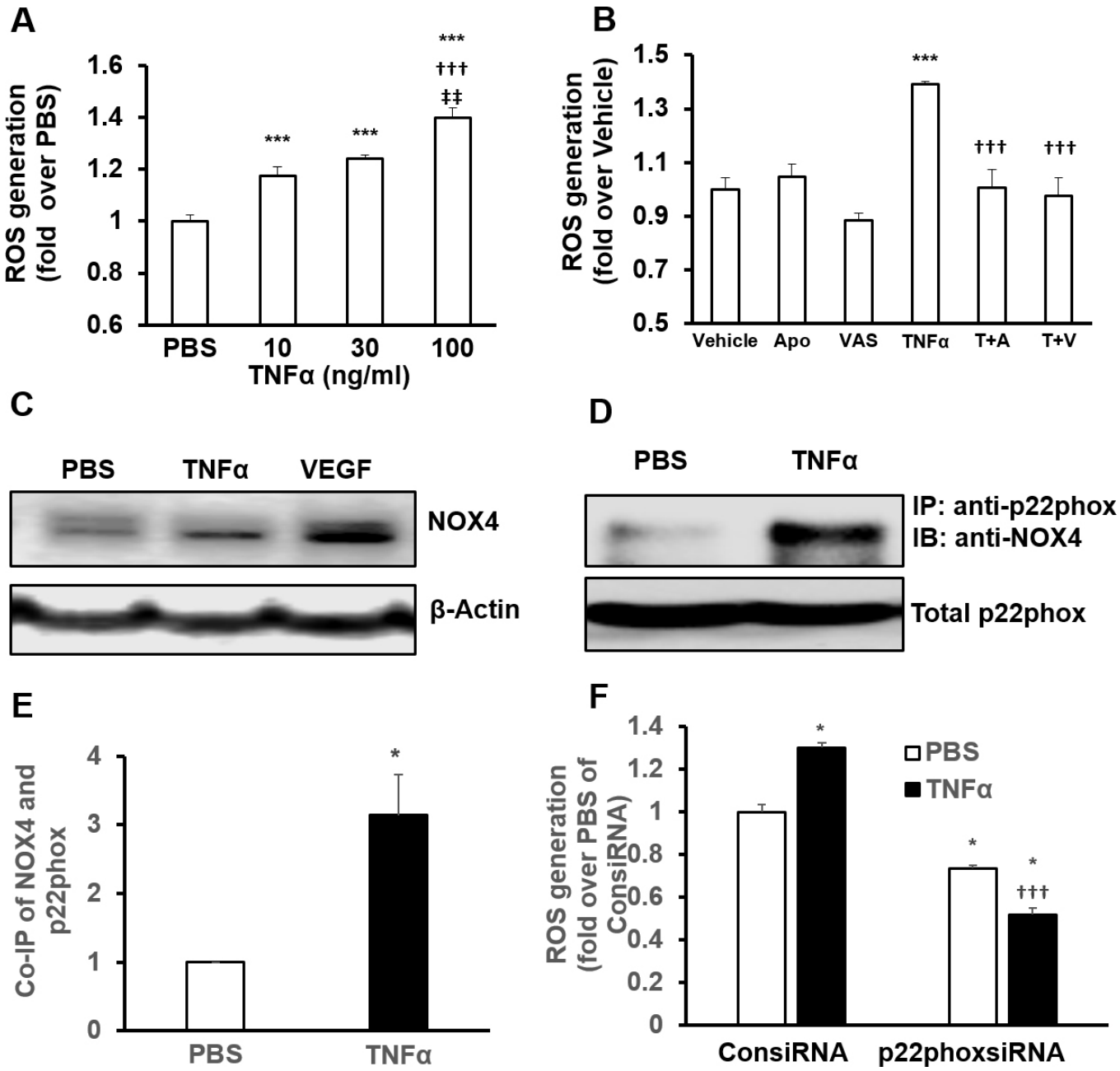

Figure 3. TNF-α induces ROS generation in human RPE cells by activating NADPH oxidase. **A**: Reactive oxygen species (ROS) generation measured with 2',7'-dichlorofluorescein diacetate (DCFDA) fluorescence in human RPE cells treated with recombinant human tumor necrosis factor alpha (TNF-α) at various concentrations for 30 min (***p<0.001 versus PBS; †††p<0.001 versus TNF-α at 10 ng/ml; ‡‡p<0.01 versus TNF-α at 30 ng/ml). **B**: ROS generation measured with DCFDA fluorescence in human RPE cells pretreated with apocynin (Apo, 100 μM) and VAS 2870 (VAS, 20 μM) for 30 min before incubation with TNF-α (20 ng/ml) for an additional 30 min (***p<0.001 versus vehicle; †††p<0.001 versus TNF-α). **C**: Western blot of NOX4. **D**: Representative gel images of coimmunoprecipitation of NOX4 and p22phox in RPE cells treated with TNF-α or vascular endothelial growth factor (VEGF) overnight (*p<0.05 versus PBS). **E**: Quantification of densitometry in RPE cells treated with TNF-α or VEGF overnight (*p<0.05 versus PBS). **F**: ROS generation measured with DCFDA fluorescence in human RPE cells) with p22phox knockdown by siRNA transfection and incubated with TNF-α (20 ng/ml) for 30 min (*p<0.05 versus PBS of ConsiRNA; †††p<0.001 versus TNF-α of ConsiRNA).

(Figure 5B). This failed to show that the NF-κB signaling pathway was involved in TNFα-induced VEGF upregulation.

Wnt/β-catenin signaling is implicated in inflammation. Activated β-catenin translocates to the nucleus and regulates gene expression by forming a complex with tissue cell factor (TCF)/lymphoid enhancing factor (LEF) transcriptional factors. Therefore, we determined whether Wnt/β-catenin signaling was involved in TNF-α-mediated VEGF upregulation. RPE cells were pretreated with JW67 [22] or XAV939 [23], inhibitors of Wnt/β-catenin signaling, before incubation with TNF-α, and the β-catenin and VEGF protein levels were measured. As shown in Figure 6A, β-catenin was increased by TNF-α as early as 1 h after treatment and was inhibited by pretreatment with XAV939, but not JW67. In the same cell lysates, VEGF protein was increased by TNF-α as early as 1 h after treatment and remained upregulated at 6 h after treatment. Inhibition of Wnt/β-catenin signaling by XAV939 prevented VEGF upregulation by TNF-α (Figure 6B). To determine the mechanism, co-immunoprecipitation of beta-catenin and TCF1 was determined. As shown in Figure 6, TNF-α treatment induced greater coimmunoprecipitated β-catenin and TCF1, and this was inhibited by pretreatment with apocynin or XAV939 (Figure 6C) or by knockdown of p22phox (Figure 6D). These findings provide evidence that TNFα led to VEGF upregulation through β catenin/TCF1 transcription.

Altogether, the results in Figure 6 and Figure 7 provide evidence that TNF-α upregulates VEGF expression in RPE cells via ROS-dependent activation of Wnt/β-catenin signaling, independent of NF-κB. These data provide evidence that TNF-α-mediated NADPH oxidase-generated ROS trigger Wnt/β-catenin activation and β-catenin

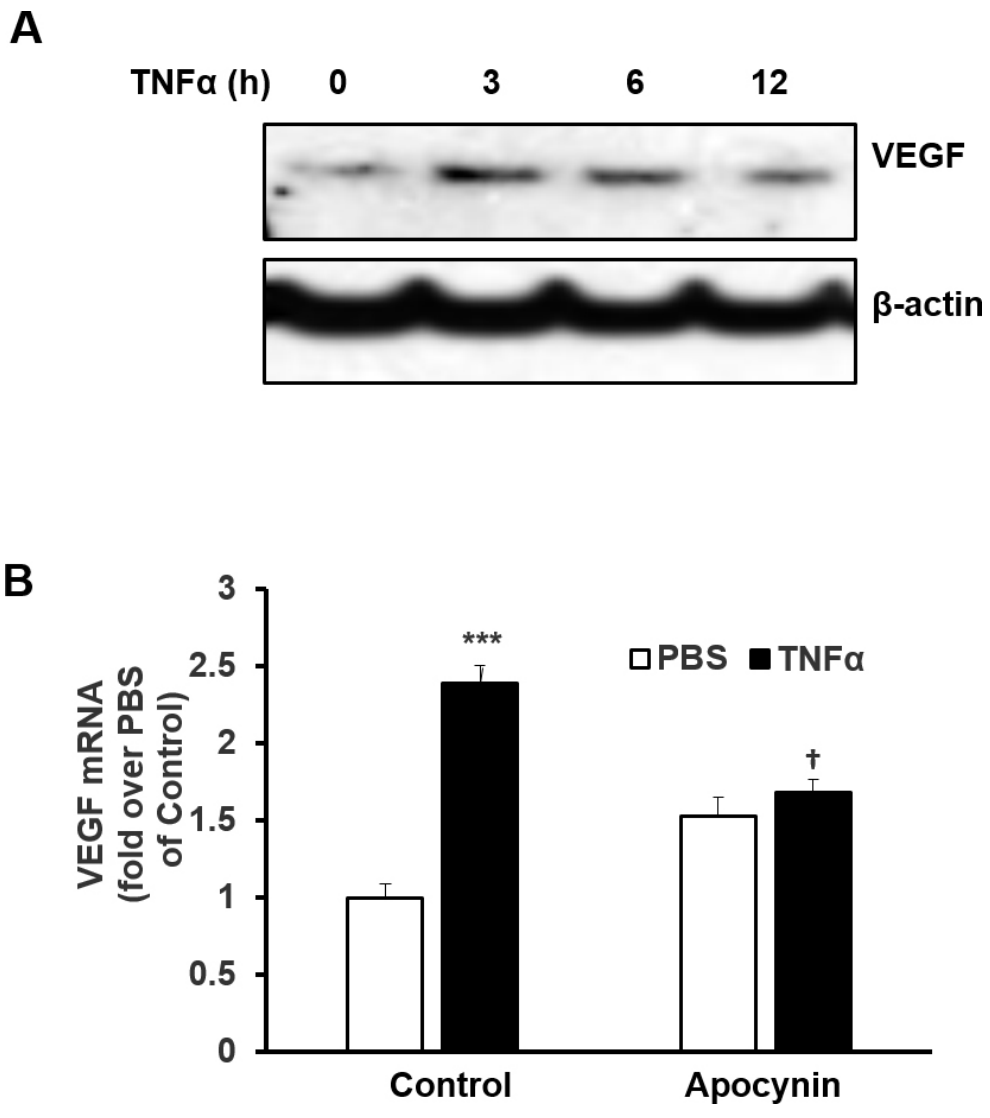

Figure 4. TNF-α upregulates VEGF expression in RPE cells via ROS-dependent signaling. **A**: Western blot of vascular endothelial growth factor (VEGF) in RPE cells treated with tumor necrosis factor alpha (TNF-α; 20 ng/ml) for 3, 6, or 12 h. **B**: Quantitative PCR of VEGF mRNA in RPE cells pretreated with apocynin (100 μM) or control for 30 min before incubation with TNF-α (20 ng/ml) for an additional 12 h (***p<0.001 versus PBS of control; †p<0.05 versus TNF-α of control).

translocation and binding with TCF1 that led to increased VEGF expression.

DISCUSSION

Neovascular AMD is often associated with CNV, in which blood vessels originate from the choriocapillaris and grow into Bruch's membrane, under the RPE or into the neural retina [24]. VEGF plays a fundamental role in the development of CNV, and anti-VEGF agents have been widely used for treatment of neovascular AMD, yielding improved vision acuity in about 40% of patients with repeated monthly injections. However, factors other than VEGF are involved in AMD. Therefore, understanding the role of these mechanisms may and lead to better treatments for neovascular AMD.

Cumulative evidence suggests that oxidative stress and inflammation play important roles in the pathogenesis of neovascular AMD [3,25]. However, the mechanisms involved in how these stresses lead to pathologic biologic events and the possible crosstalk between signaling pathways remain incompletely understood. ROS cause cell damage directly but can also trigger intracellular signal transduction that leads to various outcomes in different cell types involved in AMD. In this report, we studied the effects of the inflammatory cytokine, TNF-α, on RPE-induced VEGF expression and the interactions of inflammatory and oxidative signaling in angiogenesis, as evidenced by the development of CNV.

Using a murine model of laser-induced CNV, we found laser injury induced TNF-α expression in temporal association with the development of CNV. Inhibition of TNF-α bioactivity by an intravitreal injection of a neutralizing antibody to murine TNF-α reduced CNV volume in association with decreased VEGF expression in the RPE/choroids, compared to control. These results provide evidence that TNF-α contributed to CNV by increasing VEGF expression. VEGF is upregulated by hypoxia- or ROS-induced hypoxia

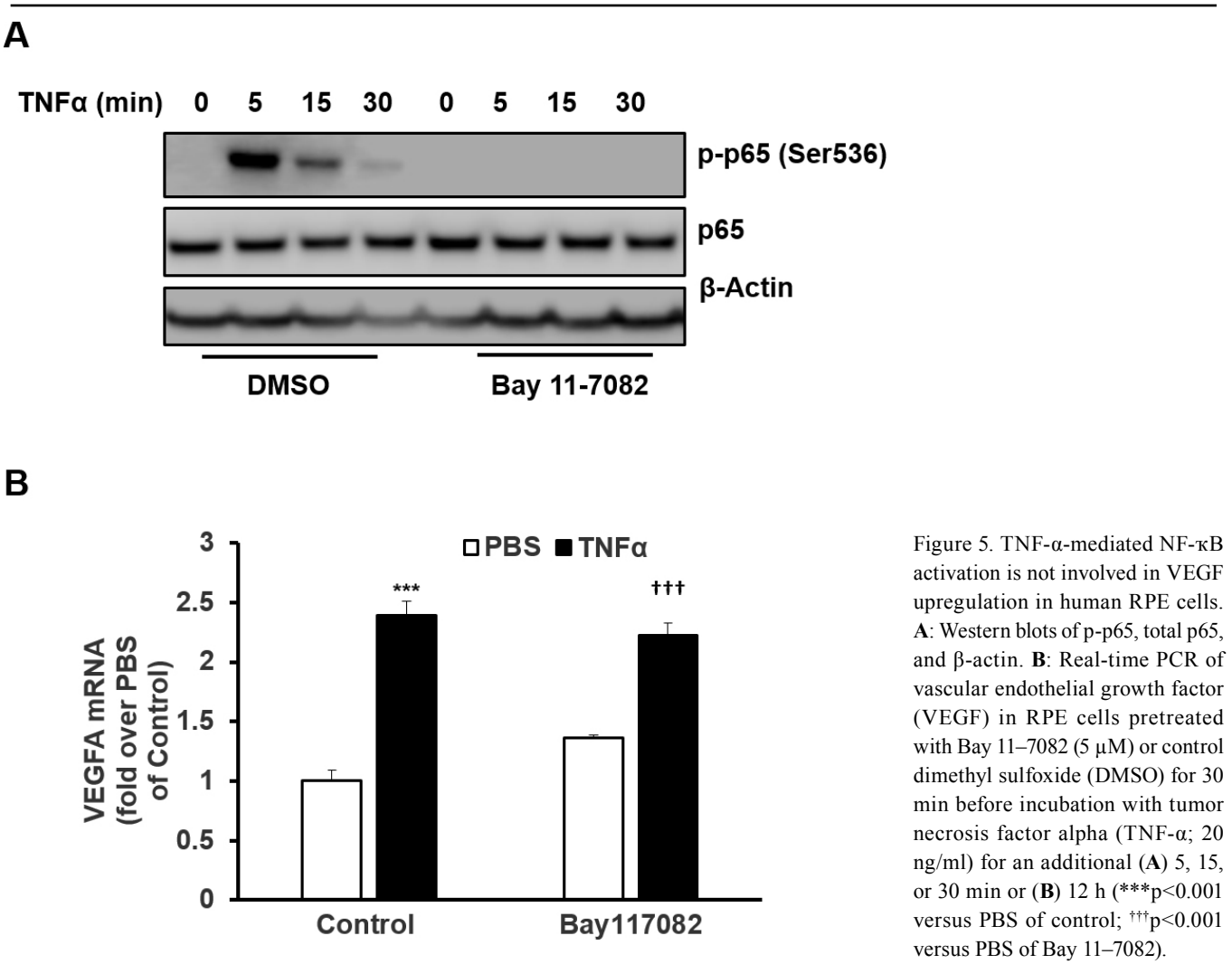

Figure 5. TNF-α-mediated NF-κB activation is not involved in VEGF upregulation in human RPE cells. **A**: Western blots of p-p65, total p65, and β-actin. **B**: Real-time PCR of vascular endothelial growth factor (VEGF) in RPE cells pretreated with Bay 11–7082 (5 μM) or control dimethyl sulfoxide (DMSO) for 30 min before incubation with tumor necrosis factor alpha (TNF-α; 20 ng/ml) for an additional (**A**) 5, 15, or 30 min or (**B**) 12 h (***p<0.001 versus PBS of control; †††p<0.001 versus PBS of Bay 11–7082).

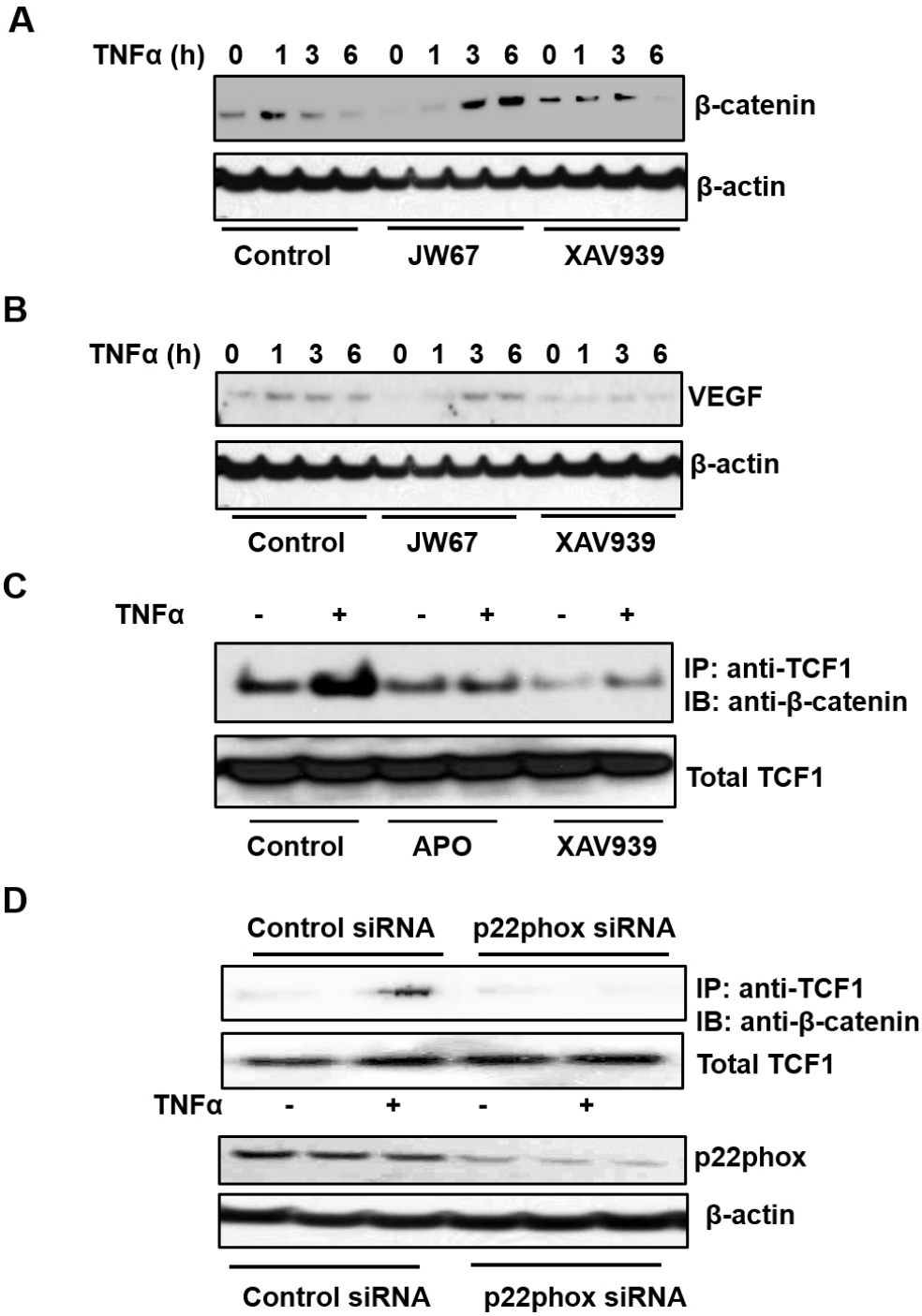

Figure 6. TNF-α upregulates VEGF by mediating ROS-dependent transcriptional activation of β-catenin. Representative western blots of (**A**) β-catenin and (**B**) vascular endothelial growth factor (VEGF) in RPE cells pretreated with JW67 (20 μM) or XAV939 (1 μM) or control dimethyl sulfoxide (DMSO) for 30 min before incubation with tumor necrosis factor alpha (TNF-α; 20 ng/ml) for an additional 1, 3, or 6 h. **C**: Coimmunoprecipitation of β-catenin and T cell factor 1 (TCF1) in RPE cells pretreated with apocynin (APO, 100 μM) or XAV939 or control DMSO for 30 min (representative blot). **D**: Coimmunoprecipitation of β-catenin and TCF1 in RPE cells transfected with p22phox siRNA and incubated with TNFα (20 ng/ml) for 2 h (representative blot).

inducible factor 1 alpha stabilization [26,27]. We found that inhibition of TNF-α activity decreased the accumulation of oxidized lipoproteins within CNV lesions, suggesting an association between inflammatory and oxidative signaling pathways that led to increased VEGF expression and angiogenesis in the form of CNV.

We delved into the signaling mechanisms surrounding TNF-α-induced intracellular ROS in regulating VEGF expression in the RPE. We report a mechanism in which the inflammatory cytokine, TNF-α, acting through NADPH oxidase-generated ROS and subsequent β-catenin transcriptional activation induced an increase in VEGF expression in RPE cells. The role of Wnt/β-catenin in neovascular AMD

has been proposed [5]. β-catenin has multiple cell functions; by interacting with cadherin, β-catenin is an adherens junction component, and β-catenin is also a component of the Wnt signaling pathway. Activated β-catenin translocates into the nucleus and associates with transcription factors from the TCF/Lef family to drive transcription of Wnt/β-catenin target genes [28]. In cultured RPE cells, TNF-α increased β-catenin expression and led to a physical association with TCF1, whereas quenching ROS by apocynin or knockdown of the NADPH oxidase subunit, p22phox, inhibited this association of β-catenin with TCF1. These results provide evidence that TNF-α-mediated Wnt/β-catenin activation was triggered by intracellular ROS. Inhibition of β-catenin by the Wnt/β-catenin inhibitor, XAV939, but not JW67, reduced TNF-α-induced VEGF upregulation in the RPE, suggesting TNF-α induced VEGF upregulation required ROS-dependent β-catenin signaling. JW67 and XAV939 efficiently inhibit transcriptional activity of β-catenin in tumor cells by binding tankyrase1/2 enzymes that stimulate β-catenin degradation. The different effects of JW67 and XAV939 in inhibiting TNF-α-mediated β-catenin expression in the RPE may potentially be due to different binding affinities to tankyrase1/2 or because of different expression levels of tankyrase1/2 in RPE cells compared to tumor cells [22]. NF-κB is a key transcriptional factor in response to TNF-α. In cultured RPE cells, TNF-α activated NF-κB; however, inhibition of NF-κB did not affect VEGF expression induced by TNF-α. Our data were consistent with findings from another study [18], in which TNF-α upregulated VEGF in a non-polarized RPE cell monolayer via an NF-κB-independent mechanism.

In summary, we demonstrated that TNF-α contributed to CNV formation by upregulating VEGF expression in RPE cells involving β-catenin transcriptional activation (Figure 7). Our results taken together provide evidence for interactions among inflammatory, oxidative, and angiogenic mechanisms and may have implications in neovascular AMD. Inhibition of TNF-α may be another means of reducing or inhibiting the pathologic effects of VEGF in the development of CNV.

ACKNOWLEDGMENTS

This work was supported by the National Institutes of Health EY014800, R01EY015130 and R01EY017011 to M.E.H., a grant from the March of Dimes 6-FY13–75 to M.E.H, a grant from the Knights Templar Eye Foundation, Inc. to H.W and an Unrestricted Grant from Research to Prevent Blindness, Inc., New York, NY, to the Department of Ophthalmology & Visual Sciences, University of Utah.

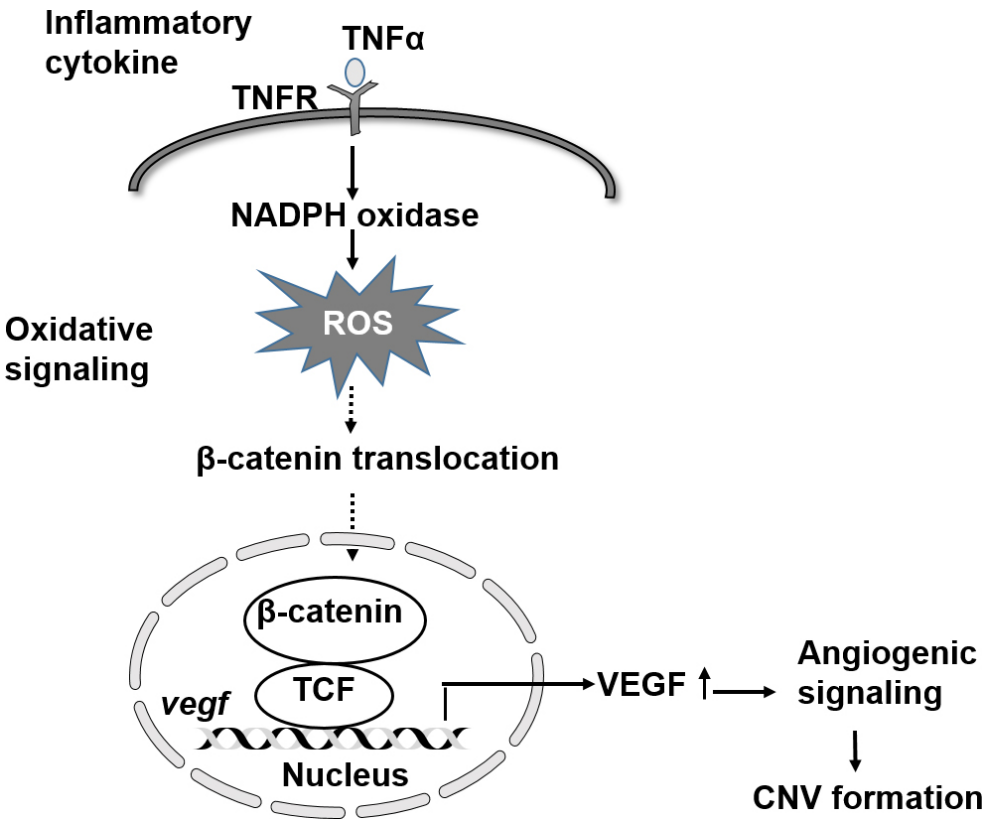

Figure 7. Diagram illustrating the hypothetical signaling pathway and interactions in inflammation, oxidative stress, and angiogenesis-regulated VEGF expression and CNV formation via activation of β-catenin (TNFR – TNFα receptor). Refer to the text for details.

REFERENCES

1. Gehrs KM, Anderson DH, Johnson LV, Hageman GS. Age-related macular degeneration merging pathogenetic and therapeutic concepts. Ann Med 2006; 38:450-71. [PMID: 17101537].
2. Bird AC. Therapeutic targets in age-related macular disease. J Clin Invest 2010; 120:3033-41. [PMID: 20811159].
3. Blasiak J, Petrovski G, Vereb Z, Facsko A, Kaarniranta K. Oxidative stress, hypoxia, and autophagy in the neovascular processes of age-related macular degeneration. BioMed Res Int 2014; 2014:768026-[PMID: 24707498].
4. Apte RS, Richter J, Herndon J, Ferguson TA. Macrophages inhibit neovascularization in a murine model of age-related macular degeneration. PLoS Med 2006; 3:e310-[PMID: 16903779].
5. Zhou T, Hu Y, Chen Y, Zhou KK, Zhang B, Gao G, Ma JX. The pathogenic role of the canonical Wnt pathway in age-related macular degeneration. Invest Ophthalmol Vis Sci 2010; 51:4371-9. [PMID: 19875668].
6. Haller JA. Current anti-vascular endothelial growth factor dosing regimens: benefits and burden. Ophthalmology 2013; 120:SupplS3-7. [PMID: 23642784].
7. Holekamp NM, Liu Y, Yeh WS, Chia Y, Kiss S, Almony A, Kowalski JW. Clinical Utilization of Anti-VEGF Agents and Disease Monitoring in Neovascular Age-Related Macular Degeneration. Am J Ophthalmol 2014; 157:825-833.e1. [PMID: 24388973].
8. Joussen AM, Bornfeld N. The treatment of wet age-related macular degeneration. Dtsch Arztebl Int 2009; 106:312-7. [PMID: 19547647].
9. Li Q, Dinculescu A, Shan Z, Miller R, Pang J, Lewin AS, Raizada MK, Hauswirth WW. Downregulation of p22phox in Retinal Pigment Epithelial Cells Inhibits Choroidal Neovascularization in Mice. Mol Ther 2008; 16:1688-94. [PMID: 18665154].
10. Monaghan-Benson E, Hartmann J, Vendrov AE, Budd S, Byfield G, Parker A, Ahmad F, Huang W, Runge M, Burridge K, Nageswara Madamanchi, M. Elizabeth Hartnett. The Role of Vascular Endothelial Growth Factor-Induced Activation of NADPH Oxidase in Choroidal Endothelial Cells and Choroidal Neovascularization. Am J Pathol 2010; 177:2091-102. [PMID: 20802176].
11. . Age-Related Eye Disease Study Research Group. A randomized, placebo-controlled, clinical trial of high-dose supplementation with vitamins C and E, beta carotene, and zinc for age-related macular degeneration and vision loss: AREDS Report No. 8. Arch Ophthalmol 2001; 119:1417-36. [PMID: 11594942].
12. Sakurai E, Anand A, Ambati BK, van Rooijen N, Ambati J. Macrophage depletion inhibits experimental choroidal neovascularization. Invest Ophthalmol Vis Sci 2003; 44:3578-85. [PMID: 12882810].
13. Hageman GS, Anderson DH, Johnson LV, Hancox LS, Taiber AJ, Hardisty LI, Hageman JL, Stockman HA, Borchardt JD, Gehrs KM, Smith RJ, Silvestri G, Russell SR, Klaver CC, Barbazetto I, Chang S, Yannuzzi LA, Barile GR, Merriam JC, Smith RT, Olsh AK, Bergeron J, Zernant J, Merriam JE, Gold B, Dean M, Allikmets R. From The Cover: A common haplotype in the complement regulatory gene factor H (HF1/CFH) predisposes individuals to age-related macular degeneration. Proc Natl Acad Sci USA 2005; 102:7227-32. [PMID: 15870199].
14. Oh H, Takagi H, Takagi C, Suzuma K, Otani A, Ishida K, Matsumura M, Ogura Y, Honda Y. The potential angiogenic role of macrophages in the formation of choroidal neovascular membranes. Invest Ophthalmol Vis Sci 1999; 40:1891-8. [PMID: 10440240].
15. Geltzer A, Turalba A, Vedula SS. Surgical implantation of steroids with antiangiogenic characteristics for treating neovascular age-related macular degeneration. Cochrane Database Syst Rev 2013; 1:CD005022-[PMID: 23440797].
16. Markomichelakis NN, Theodossiadis PG, Sfikakis PP. Regression of neovascular age-related macular degeneration following infliximab therapy. Am J Ophthalmol 2005; 139:537-40. [PMID: 15767068].
17. Theodossiadis PG, Liarakos VS, Sfikakis PP, Vergados IA, Theodossiadis GP. Intravitreal administration of the anti-tumor necrosis factor agent infliximab for neovascular age-related macular degeneration. Am J Ophthalmol 2009; 147:825-30. [PMID: 19211094].
18. Terasaki H, Kase S, Shirasawa M, Otsuka H, Hisatomi T, Sonoda S, Ishida S, Ishibashi T, Sakamoto T. TNF-alpha decreases VEGF secretion in highly polarized RPE cells but increases it in non-polarized RPE cells related to crosstalk between JNK and NF-kappaB pathways. PLoS One 2013; 8:e69994-[PMID: 23922887].
19. Lichtlen P, Lam TT, Nork TM, Streit T, Urech DM. Relative contribution of VEGF and TNF-alpha in the cynomolgus laser-induced CNV model: comparing the efficacy of bevacizumab, adalimumab, and ESBA105. Invest Ophthalmol Vis Sci 2010; 51:4738-45. [PMID: 20393113].
20. Wang H, Geisen P, Wittchen ES, King B, Burridge K, D'Amore PA, Hartnett ME. The Role of RPE Cell-Associated VEGF189 in Choroidal Endothelial Cell Transmigration across the RPE. Invest Ophthalmol Vis Sci 2011; 52:570-8. [PMID: 20811045].
21. Wang H, Yang Z, Jiang Y, Hartnett ME. Endothelial NADPH oxidase 4 mediates vascular endothelial growth factor receptor 2-induced intravitreal neovascularization in a rat model of retinopathy of prematurity. Mol Vis 2014; 20:231-241. [PMID: 24623966].
22. Waaler J, Machon O, von Kries JP, Wilson SR, Lundenes E, Wedlich D, Gradl D, Paulsen JE, Machonova O, Dembinski JL, Dinh H, Krauss S. Novel synthetic antagonists of canonical Wnt signaling inhibit colorectal cancer cell growth. Cancer Res 2011; 71:197-205. [PMID: 21199802].
23. Huang SM, Mishina YM, Liu S, Cheung A, Stegmeier F, Michaud GA, Charlat O, Wiellette E, Zhang Y, Wiessner S, Hild M, Shi X, Wilson CJ, Mickanin C, Myer V, Fazal A,

Tomlinson R, Serluca F, Shao W, Cheng H, Shultz M, Rau C, Schirle M, Schlegl J, Ghidelli S, Fawell S, Lu C, Curtis D, Kirschner MW, Lengauer C, Finan PM, Tallarico JA, Bouwmeester T, Porter JA, Bauer A, Cong F. Tankyrase inhibition stabilizes axin and antagonizes Wnt signalling. Nature 2009; 461:614-20. [PMID: 19759537].

24. Hartnett ME, Elsner AE. Characteristics of exudative age-related macular degeneration determined in vivo with confocal and indirect infrared imaging. Ophthalmology 1996; 103:58-71. [PMID: 8628562].

25. Telander DG. Inflammation and age-related macular degeneration (AMD). Semin Ophthalmol 2011; 26:192-7. [PMID: 21609232].

26. Bazan NG, Lukiw WJ. Regulation of vascular endothelial growth factor (VEGF) gene transcription by insulin growth factor (IGF) and hypoxia inducible factor (HIF) in mouse retina undergoing neovascularization. Invest Ophthalmol Vis Sci 1999; 40:B5111-.

27. Semenza GL, Agani F, Iyer N, Kotch L, Laughner E, Leung S, Yu AM. Regulation of cardiovascular development and physiology by hypoxia- inducible factor 1. Ann N Y Acad Sci 1999; 874:262-8. [PMID: 10415537].

28. Valenta T, Hausmann G, Basler K. The many faces and functions of beta-catenin. EMBO J 2012; 31:2714-36. [PMID: 22617422].

Articles are provided courtesy of Emory University and the Zhongshan Ophthalmic Center, Sun Yat-sen University, P.R. China. The print version of this article was created on 3 February 2016. This reflects all typographical corrections and errata to the article through that date. Details of any changes may be found in the online version of the article.